



Effect of Mg Addition on Morphology, Roughness and Adhesion of Cr Chromized Layer Produced by Pack Cementation

S. Djemmah^{*a,b}, Y. Madi^a, M. Voué^b, A. Haddad^c, D. Allou^c, S. Ouallam^c, H. Bouchafaa^a, A. Rezzoug^c

^a University of Science and Technology Houari Boumediene, Laboratory of Technology of Materials (LTM), Algeria

^b University of Mons, Physics of Materials and Optics Unit (LPMO), Research Institute for Materials Science and Engineering, Belgium

^c Research Center in Industrial Technologies (CRTI), Algeria

PAPER INFO

Paper history:

Received 24 May 2023

Received in revised form 19 June 2023

Accepted 20 June 2023

Keywords:

Magnesium Doping
Chromium Chromizing
Surface Roughness
Strength Adhesion

ABSTRACT

In the present study, the effect of adding Magnesium (Mg) as a doping element on the morphology and surface characteristics of the chromized layer was investigated. To achieve this, chromized layers were coated and doped by a chromizing process in pack-cementation at 1050°C. The thickness of the doped layer was about 26 µm, whilst chromized was approximately 24 µm. The surface morphology and composition of the coatings were analyzed using scanning electron microscopy (SEM) and energy dispersive X-ray spectroscopy (EDX). The results showed that a crystalline structure can be successfully deposited by adding Mg as a doping element to the pack mixture. Therefore, Mg acts as a barrier against Cr₂O₃ formation, resulting in a more rich-chromium-zone and forming protective oxide. Moreover, less carbide is formed in the doped layer. The roughness of the layer is enhanced by adding Magnesium (Mg) and it has a lower average roughness (Ra) 3 times than that of chromized, of about 0.315 µm and 1.039 µm, respectively. In addition, progressive loading scratch was performed at 1N and 20N. The results demonstrated that Mg in the chromized layer increases the ability to with-stand varying levels of mechanical stress with strength adhesion of about 19.21N and can be more protective than Cr chromized.

doi: 10.5829/ije.2023.36.10a.05

NOMENCLATURE

Wt%	weight	SEM	Scanning electron microscope
Ra	Average roughness	EDX	Energy-dispersive X-ray spectroscopy
Rz	Mean height roughness	Er	Elastic recovery ratio
Rd	Residual depth	2D	two-dimensional
Pd	Penetration depth	3D	three-dimensional
Lc	Critical load		

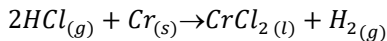
1. INTRODUCTION

In industrial applications, materials must be resistant to environmental attacks such as corrosion, stress, wear and fatigue. Especially when they are applied to applications that requires high temperature applications. However, stainless steels have been used for environments such as petrochemical or electric utility fluidizing particles and any hydrogen halide as the plants [1, 2]. They are a popular choice for their low cost and their physical and mechanical properties [3, 4], despite this they remain of

poor quality in front of many aggressive factors. Among these stainless steels, citing the ferritic steel (AISI 430) which has been found in previous studies to be less resistant to oxidation at high temperatures [5, 6]. To overcome these limitations, surface coatings have been widely employed as an effective means of improving material performance in such environments. One of the surface modification methods frequently employed is diffusion coating through the chromizing process in pack cementation to enrich alloy surfaces with chromium (Cr) [7-9]. However, in chromizing process, the chromium

*Corresponding Author Email: sdjemmah@usthb.dz,
sarah.djemmah@umons.ac.be (S. Djemmah)

(Cr) is used as a master alloy where it contributes to improving in many properties of the coated material due to its excellent hardness, wear resistance, and corrosion resistance [10]. On the other hand, during the high temperature chromizing process the activator usually ammonium chloride (NH_4Cl); presents in the mixture is decomposed into hydrogen chloride (HCl), nitrogen (N_2), and hydrogen gas (H_2). The HCl formed during this process reacts with the chromium present in the pack according to the following reaction [11]:



This reaction is crucial to the formation of the desired chromizing coating. At temperatures around 1000°C , the interaction between chromium and free carbon (C) found in the stainless steel substrate can lead to the formation of chromium carbides such as Cr_7C_3 , $(\text{Cr,Fe})_7\text{C}_3$ and Cr_{23}C_6 on the surface of the metal coated [12-14]. These carbides can enhance wear resistance and give high hardness [15, 16], on the other side they act as a diffusion barrier, restricting the growth of a metallic Cr-rich layer which causes the failure adherence of the layer [17]. Consequently, a decarburized zone can develop below the coating. On the other hand, one of the challenges encountered in the chromizing process is the occurrence of voids, which can arise due to the Kirkendall effect during pack cementation [18, 19]. Additionally, the presence of carbides and intermetallic phases, which occur due to the diffusion reactions, may introduce variations in the topography of the coating and increasing the surface roughness [20, 21]. This undesirable consequence may comprise the functional characteristics of the coated surface [22]. They can also weaken the adhesion of the chromized layer, leading to delamination and durability. The formation of the chromium oxide such as Cr_2O_3 by introduction some oxygen (O) in the pack mixture can enhance the hot oxidation behavior when is exposed to hot damaged environments where they found that retardation in formation of the Cr_2O_3 oxide can lead the increase of the formation of non-protective oxides [23]. Beside this the Cr_2O_3 is known for its relatively low adhesion to the substrate, which can result in poor bonding between the coating and the substrate. This low adhesion can cause delamination to the coated surface, reducing the durability and longevity of the chromizing coating. Additionally, Cr_2O_3 has a relatively high coefficient of thermal expansion compared to the substrate material, which can induce thermal stress and strain within the coating [24]. To address this challenge, turning to the process pack cementation, wherein the addition of dopant elements and substitutions to the mixture cementation pack can alter its properties and improve surface characteristics. The element magnesium (Mg) can be used as a catalyst in the production of chromium hydroxides and oxides at high temperatures, including Mg_xCr_y , oxides which are

considered stable, resistant and auto-protective [25].

Mg element can refine the grain size of chromized layers with coarse grain structure, improving the mechanical properties and potentially reducing roughness. It is thought that magnesium (Mg) dopant may act as a reducing agent, therefore reducing Cr_2O_3 formation and enhancing the Chromium (Cr) diffusion into the substrate, which would then achieve a more uniform and adherent layer and reduce roughness in the chromized layer [26, 27].

Based on our review of the literature, there has been no research on the chromized chromium by pack cementation method, doping with magnesium (Mg) substitution. This study aims to investigate the effect of Magnesium (Mg) addition on the microstructure, morphology and enhancement of surface conditions of the chromized layer on the AISI 430 obtained through chromization process in pack cementation by reducing the formation of intermetallic phases and carbides hence, replaced by protective oxides. Additionally, the study aims to explore the potential of small amounts of magnesium (Mg) for substituting chromium (Cr) oxides and enriching the surface with chromium (Cr). Furthermore, the findings of this study may contribute to the development of advanced chromization technique with enhanced surface properties, contributing a better resistance against delamination, spallation, adhesive and failure and benefitting various industrial applications.

2. MATERIALS METHOD

In this study, Cr-Mg alloy was coated on the surface of AISI 430 Ferritic stainless steel ($10 \times 10 \times 1$) mm^3 using the chromizing process in pack-cementation, by adding a Mg content as a doping element to the Cr pack mixture. The substrates were ground before proceeding coating using mechanical polishing (up to #1000 SiC grit), immersed in acetone solution (for 10 min) and cleaned by an ultrasonic bath. Each sample was placed inside an alumina (Al_2O_3) crucible that could withstand high temperatures (up 1800°C) in two pack mixture (with and without Mg doping element). Thus, they were dipped in a powder mixture containing Cr, NH_4Cl , Al_2O_3 , for the first coating and Cr, NH_4Cl , Al_2O_3 , and Mg for the second coating. The weight ratio of the components of the Cr chromized and Cr (3wt.% Mg) doped coatings is summarized in Table 1.

The crucibles (powder pack and samples) were not passed through a glove box but were placed directly into the furnace to provide a small amount of oxygen (the fast irreversible incorporation). As a safety precaution, the crucible was sealed with lid to not allow the powder spreads in the furnace when injecting Argon (Ar) gas, then placed in the CARBOLITE tubular furnace (Carbolite TZF 12/100/-900, Hope Valley, UK). The crucibles (samples and pack mixture) kept in the furnace at room

temperature ($25^{\circ}\text{C} \pm 1$) under Argon gas injection, keeping the outlet of the furnace open to ensure that most gases were eliminated and escaped from the system then the tube furnace outlets were closed in order to proceed with the coating process (see Figure 1). The treatment was prepared with a heating rate of $6^{\circ}\text{C}/\text{min}$ and kept this heating rate value during all the coating process. The samples were not prepared in a glove box to ensure a small quantity of oxygen that will interact with the powder, knowing that the gases and oxygen escaped will be removed by argon injection.

During the chromizing process, the temperature was reached 50°C at the beginning and held at this value for 1h. This was to avoid thermal shock, which damages the crucible. On the other hand, to provide that the starting temperature is uniform throughout the surface and allows for a controlled and consistent heating process. Afterward, the temperature was increased to 1050°C ($6^{\circ}\text{C}/\text{min}$), and then held for 8 hours in a furnace under Argon (Ar) injection. For cooling down, the samples were kept in the furnace under Argon gas and then they removed.

Investigation of the morphology and composition of the Cr and the Cr-Mg coated alloy was evaluated using a HIROX SH-3000 Desktop scanning electron microscope (SEM) (HIROX, Tokyo, Japan), integrated with energy dispersive X-ray spectroscopy (EDX) BRUKER/AXSI. Thus, the coating surfaces were metalized with conductive layer of gold (Au) before scanning

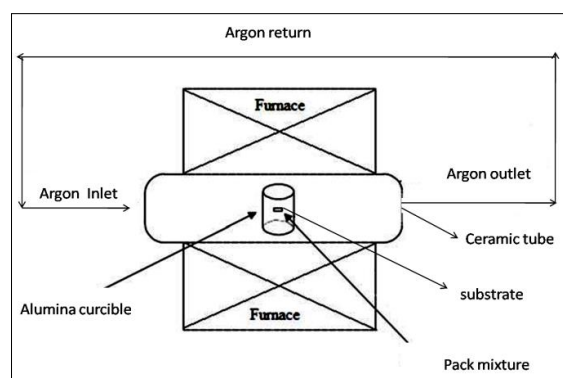


Figure 1. Explanatory schematic of the chromizing process setup

TABLE 1. Composition and content of chromized pack mixtures

Component	Content (wt.%)	
	Cr coated	Cr-Mg Coated
Cr	20	20
Al_2O_3	75	72
NH_4Cl	5	5
Mg	/	3

electron microscopy, which accounted for the appearance of gold (Au) peaks in the EDX spectrum. The metallization was performed with Denton Vacuum Desk V (Denton Vacuum, Philadelphia, USA). A non-contact optical profilometer type WYKO NT1100 (*Sensofar, Terrassa, Spain*) with a magnification objective of $20 \times$ NA 0.15; was utilized to measure the roughness without scratching the coated layers (Cr and Cr-Mg). Adhesion of the coatings was evaluated using a progressive linear scratch test in range of about 1 to 20N. Therefore, tests were performed using a CSM scratch instrument (*CSM Instruments SA, Peseux, Switzerland*). The parameters are shown in Table 2. Moreover, the scratch track was analyzed by optical microscopy type Nikon Eclipse LV100ND (*Nikon instruments, Tokyo, Japan*).

3. RESULTS AND DISCUSSION

3. 1. Microstructure and Phases Investigations

Figure 2 represents SEM micrographs of Cr and Cr-Mg coated surfaces. As can be seen, the chromized surface without Mg adding represents almost uniform darker rough structure, while a small particules were observed in lighter color with a non-uniform distribution along the surface. This particules could be Cr oxides such as Cr_2O_3 and carbides [28]. Thus, the darker region can present the chromium-rich region (Figure 2(a)) distributed across the treated surface. Moreover, no cracks were visible on the surface of the Cr chromized. However, it is known that the deposition of Cr_2O_3 in some parts of the Cr coated may lead to the apparition of cracks. Moreover, some pores have been observed and according to the studies conducted by Fan et al. [29], the kirkendall effect was found to be responsible for pores and voids formation in chromizing coatings.

In order to determine the thickness of chromized coatings, three measurements were taken with optical microscopy for each coating. The thickness was confirmed with a contact profilometer with a diamond stylus that was moved vertically and laterally in contact with the coating to measure the thickness. However, the thickness of the coatings was performed by Cr and Cr doped with 3%.wt Mg coatings had a thickness about of $24.82\mu\text{m}$ and $26.91\mu\text{m}$, respectively.

In Figure 2(b), the structure of Cr doped with 3 wt.% Mg is shown. The SEM image shows crystalline microstructure with a non-uniform distribution of particles size. The aspect appears lighter and smoother than Cr chromized surfaces, where grain can be seen in

TABLE 2. Scratch test parameters under progressive load

Load (N)	Indenter type, R (μm)	sliding speed (mm/min)	Length of the scratch (mm)
[1-20]	Diamond Rockwell C, 200	38	4

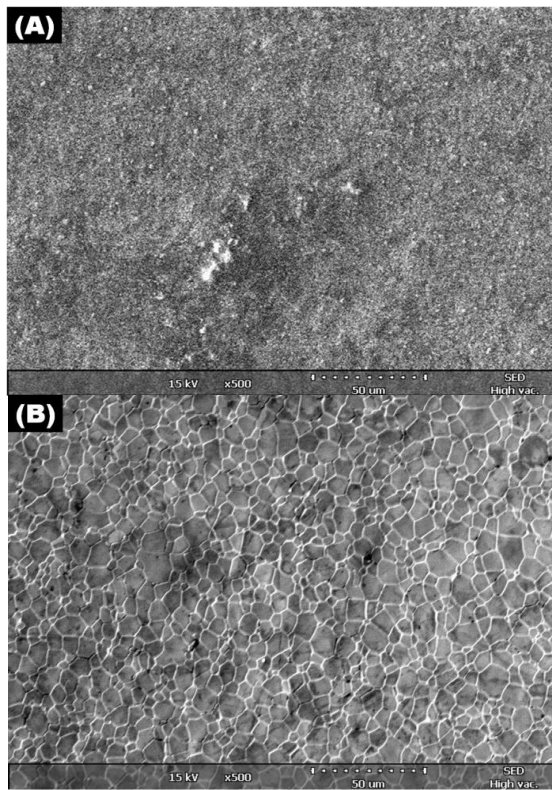


Figure 2. SEM micrographs of coated layer (top surface) deposited by chromizing process in cementation pack under Argon gas at 1050 °C for 8h: (A) Cr chromized; (B) Cr-Mg doped coating

grey with boundaries in lighter color. The growth of this crystalline structure can be explained by the fact that the coating develops crystal structure and new phases as a result of solid-state transformation occurring during the chromizing process at high temperature such as 1050°C. Subsequently, the state solid-state diffusion can exhibit movement, migration and rearrangement of the atoms through the solid-state diffusion due to the concentration gradient and causes the growth of this crystalline structure.

An EDX analysis along the surface of the Cr and Cr-Mg coatings is shown in Figure 3. The EDX spectra in the two coatings show an intense peak of Cr, indicating that Cr is deposited on the surface, resulting in Cr-rich regions that form more easily at higher Cr content [30]. Furthermore, the presence of Mg and O in the Cr-Mg doped was also confirmed by the EDX scanline (Figure 3(b)), where the O peak appears in the Cr chromized is more intense than that of Cr doped due to the formation of Cr₂O₃ in its surface (Figure 3(a)). It suggests that the magnesium (Mg) could potentially react at high temperature with the chromium (Cr) of the master alloy to form a layer containing oxides such as magnesium chromium (MgCr₂O₄) and forming this phase with a small amount in the chromized structure. Thus, it acts as a

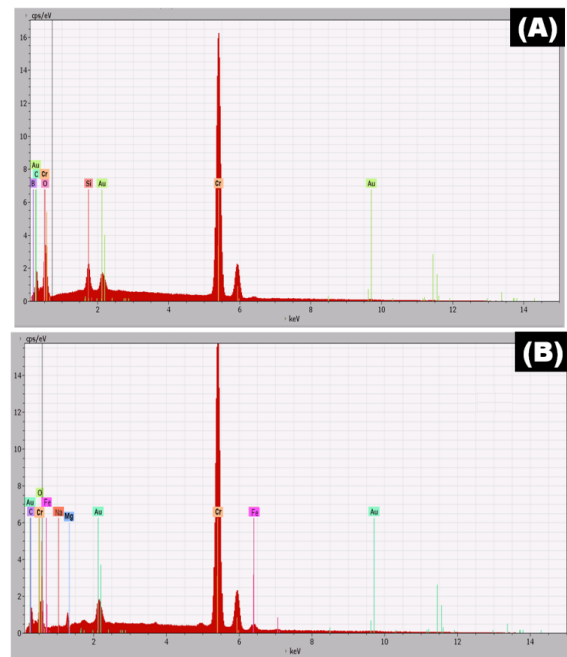
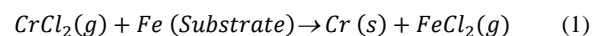


Figure 3. EDX spectrum of the coated layers: (A) Cr chromized surface; (B) Cr doped with 3wt. % Mg

barrier against Cr₂O₃ formation hence enriches the surface of the metallic Cr. Our EDX results are in agreement with the findings of Jafarnejad et al. [31] and Abbasi et al. [32], where they studied the composition of the MgCr₂O₄ oxide by the XRD and EDX analysis. Whereas, a minor amount of iron (Fe) and carbon (C) were observed, it is related to the diffusion of the 430 SS substrate, which reacted during the chromizing process to form probably intermetallic compounds such as (Cr,Fe)₇C₃, Cr₇C₃ and Cr₂₃C₆. They had FCC crystalline structures [33] and they precipitate at the grain boundaries with different amounts in the chromized and doped layer according to the previous studies [34]. These carbides enhance hardness and increase roughness because they are considered as brittle phases [35].

On the other hand, the Cr and Cr-Mg coatings do not contain any chlorine impurities left over from the chemical reactions occurring during the chromizing process at 1050°C. However, the chromized surface is composed only of rich chromium (Cr), chromium carbides and Cr₂O₃ oxide, while Cr-Mg revealed more chromium-rich zones and a small amount of Mg oxide.

In previous studies by Zheng and Rapp [36], they have reported that during the chromizing process and at a temperature about of 880°C, the substrate is subjected to weight loss due to the evaporation of the volatile FeCl₂ which reacts with the substrate by diffusion, resulting in porous coating. The formation of volatile FeCl₂ could be produced by the following chemical reaction [37]:



The results shown in Table 3, represent the weight measure of the substrate before and after the chromizing process. The results demonstrate an increase of the weight gain after chromizing, which may confirm the absence of volatile FeCl_2 in the coated surfaces and that they have not undergone mass consumption [37]. In addition, Cr-Mg chromized showed an increase of 0.0436 g over that of Cr chromized (0.0247 g). This affirms the role of Mg addition in the formation of rich-chromium (Cr) and decrease the formation of carbide in the chromium layer by diffusion process into the substrate.

3. 2. Surface Topography The surface roughness parameters, a direct extension of the line roughness parameters, are commonly used in optical profilometry to describe the topography of chromized coatings. The roughness can be expressed as:

$$R_a = \frac{1}{A} \iint_A |z(x, y) - \bar{z}| dx dy \quad (2)$$

where $z(x, y)$ represents the height, and \bar{z} is the average of height over the surface area (A). The measurement of average roughness (R_a) and mean roughness height (R_z) were recorded using a non-contacter profilometer. Results are shown in Table 4.

Figure 4 represents 2D images of Cr and Cr-Mg chromized coatings. It can be seen from Figure 4-A and B, that the texture of Cr-Mg (3 wt.%) is different to that of Cr chromized (Figure 4(b)). It can be justified by the presence of particles and its non-uniform distribution, they have been observed previously by the SEM analysis (Figure 2(a) and Figure 4(a)). These particles are considered as an intermetallic phase which has a different structure from the Cr. This leads to the increase of the roughness on the surface and causing the clustered morphology within a microscopic regime observation (3D image: Figure 4(c)). Clusedted morp-hology is due to solid-state diffusion and chemical reactions occurring that

TABLE 3. Measurements of weight changes before and after chromizing process

Coating	Weight (g)	
	Before chromizing	After chromizing
Cr	0.9245	0.9164
Cr-Mg (3wt.%)	0.9492	0.960

TABLE 4. Surface roughness parameters for the Cr chrom-ized and Cr doped coatings reported for 20x magnification

Sample	Roughness parametrs (20x NA 0,15)	
	R_a [μm]	R_z [μm]
430-SS	1.918	9.348
Cr coated	1.039	7.834
Cr-Mg coated	0.315	5.803

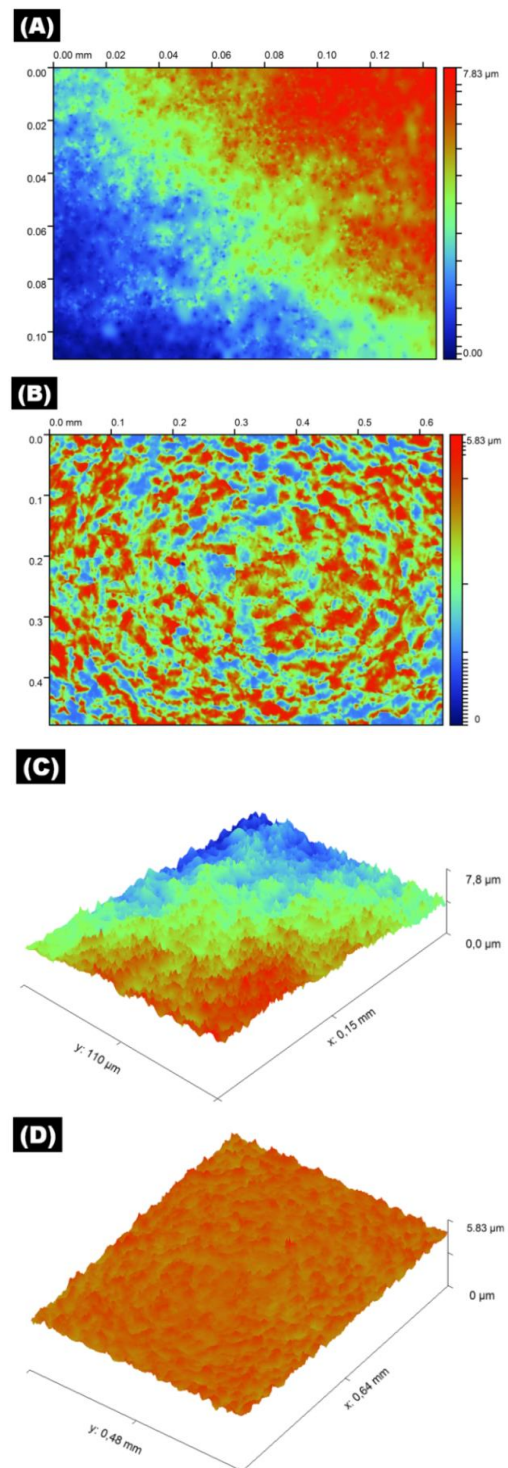


Figure 4. 2D and 3D optical profilometer images: (a), (c) Cr chromized surface; (b), (d) Cr doped with Mg surface

occur during the chromizing process, which can affect the surface characteristics hence its mechanical properties. Deposition of Cr_2O_3 can also increase the roughness of the coated substrate [38].

The distribution of the Cr-Mg surface is more uniform

and it did not show topological defects (Figure 4(d)), such as particles inclusions, asperities, pores and voids which may explain the smoothness of the surface ($R_a = 0.315 \mu\text{m}$) [39], it can be related to the characteristics of the mixture pack used in this chromizing process [20], where the dopant element (Mg) may act as a particulates refiner.

In the absence of Mg dopant, the roughness of the Cr chromized surface increased three times about of $1.039 \mu\text{m}$, compared to the doped Cr-Mg, which showed an average roughness about of $0.315 \mu\text{m}$. The Mg improves the roughness of 430 SS six times compared to its initial state ($R_a = 1.918 \mu\text{m}$). According to Hou and Kang [40], coatings containing Mg oxides could have a rough surface. Whereas, it has been found that doping with Mg decrease the surface roughness [26].

3. 3. Adhesion Testing

The adhesion of the layers was investigated by a progressi-ve scratch test, gradually increasing the loading force from 1N to 20N applied load. This scratched the coating surface with a loading rate of 38 N/min. Hence, it caused a scratch length of 4mm (Table 2). However, different behavior can be exhibited in the recorded diagram of penetration depths (Rd and Pd) of the Cr (Figure 5(a)) and Cr-Mg (Figure 5(b)) chromized layers. The first critical load (L_{c1}) of the Cr chromized was observed at $L_{c1} = 3.91\text{N}$, at which point cracks occurred during scratch loading. The initial observed critical load of the Cr doped with Mg was about $L_{c1} = 7.32\text{N}$, revealing minor cracks at this stage. It is considered a lower critical load according to the studies of Lee et al [7].

Considering that the recorded critical load (determined by L_c) may be considered as an indicator of strength adhesion and adhesion failure [41]. Accordingly, the Cr chromized at the second and third recoded critical load; $L_{c2} = 7,75\text{N}$ and $L_{c3} = 15.85 \text{ N}$, respectively. showed a significant and visible damage corresponding to the occurrence delamination failure and the beginning of the pull-off of the layer from the coated surface. Though the Cr doped resisted until $L_{c2} = 19.21 \text{ N}$ and did not show any delamination, it experienced plastic deformation despite that. The adhesion strength is classified as HF1 an excellent quality for the Cr-Mg doped, indicating that Cr doped exhibits no detachment or delamination when subjected to scratch test, while the Cr chromized is classified as HF2 .

The trends of the penetration depth (Pd) and residual depth (Rd) were similar until averaged to $20 \mu\text{m}$, then increased and averaged approximately $140 \mu\text{m}$ after the critical load $L_{c3} = 15.85 \text{ N}$ (Figure 5(a)). This behavior can be explained by the fact that the Cr chromized experienced a failure mode at this critical load (L_{c3}), which caused the increase in Pd and Rd values. The increase of the penetration depth is caused by the rough surface conditions and by the crack formation after subjecting to the scratch test.

On the other hand, the trends of Pd and Rd profiles

for the Cr-Mg doped remain stable and uniform where its penetration depth (Pd) increased at a maximum depth value of $32 \mu\text{m}$ and Rd practically increased with a very low trend (Figure 5(b)), but still lower than those of the Cr chromized (Figure 5(a)). This result, can be attributed to the uniform and smooth fine matrix and surface of the Cr-Mg doped (Table 4), which could limit the amount of

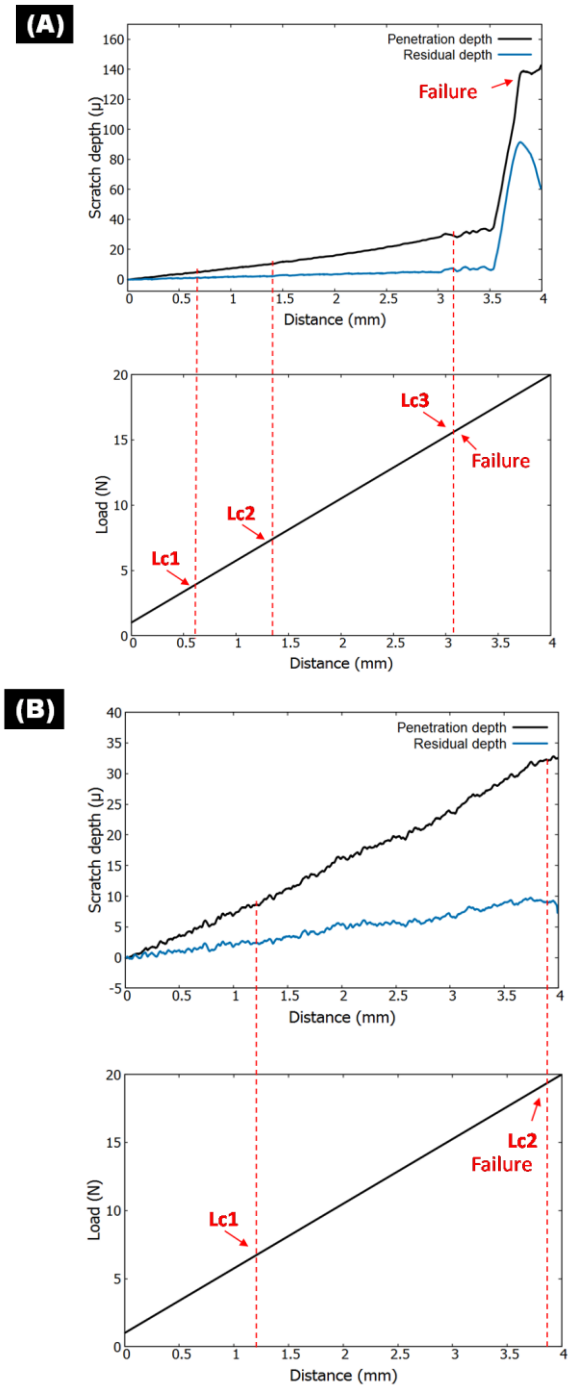


Figure 5. Plot of penetration depths after scratch progressive test under load range of 1 to 20N: A- Cr chromized; B- Cr-Mg doped

penetration and residual deformation that occurs before failure and remain the surface to be more resistant to deformation .

Elastic recovery ratio Er (%) is one of the physical properties describing viscoelastic surfaces. (Er) can be calculated by the following equation:

$$Er \% = \frac{Pd - Rd}{Pd} \times 100 \quad (3)$$

where, Pd is the penetration depth and Rd is the residual depth measured against the applied load.

The results of the elastic recovery ratio (Er) measured for the chromized coating tested are shown in Table 5. The results reveal that the highest elastic recovery ratio (Er) is recorded for the Cr-Mg chromized surface, and it indicates an excellent viscoelastic behavior of the coated surface compared with that of Cr chromized.

Figure 6 show optical microscopic observations of scratch tracks. The surface of the Cr chromized was dark so it was hard to create the proper reflection to the recorded image at high resolutions (high magnifications) hence the image of scratch track showed a lighter area

TABLE 5. Depth penetration measurements after scratch test

Coating	Scratch parametrs		
	Pd [μ m]	Rd [μ m]	Er [%]
Cr chromized	141	60	57.85
Cr-Mg chromized	32	7.5	76.56

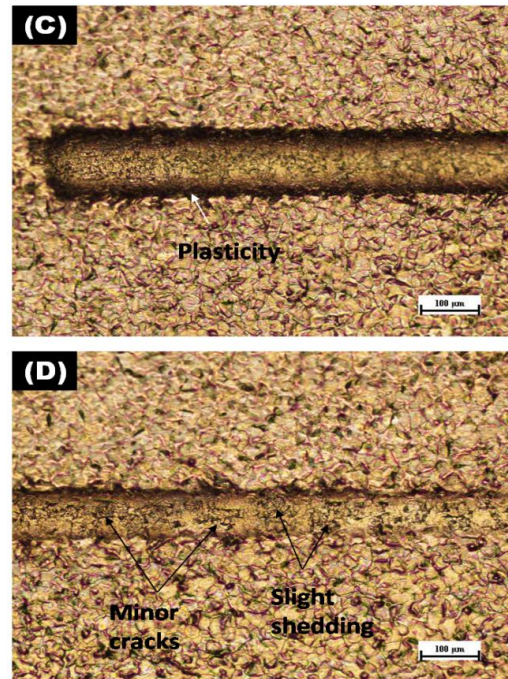
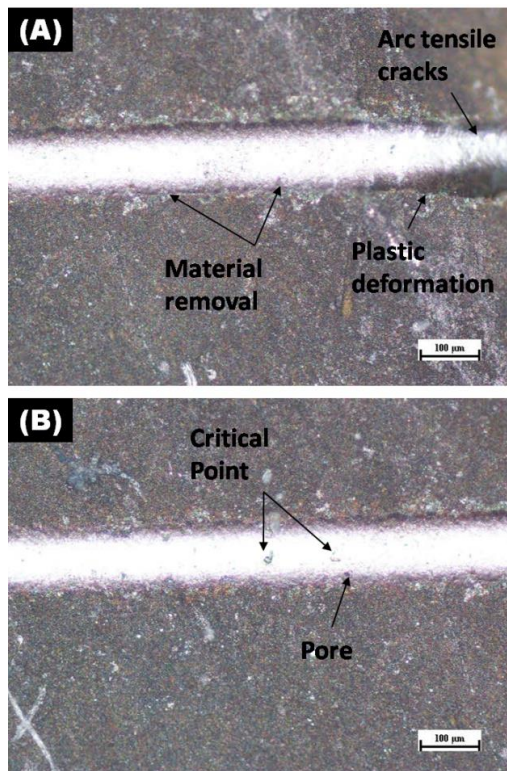


Figure 6. Optical micrographs of scratch tracks after 1-20 N applied progressive load: (A) Cr chromized; (B) Cr-Mg chromized

(Figure 6(a) and (b)). The scratch test trace of the Cr-Mg chromized showed tiny minor cracks at the first critical load $L_{C1} = 7.32$ N (Figure 6(d)), while a plasticity at the edge area and very slightly shedding were observed. It indicates that the Cr-Mg layer in response to the applied progressive load varying from 1N to 20N, deforms plastically without fracture, delamination or material removal (Figure 6(c)). However, the Cr-Mg (3wt.%) doped layer tends to have a high resistance to plastic deformation. This means that the surface can recover its shape easily and its less subject to permanently deformed or damaged by the scratch test. As shown in Table 5, the doped layer exhibited an excellent elastic recovery ratio of about $Er = 76\%$. Despite this, very small areas of shedding caused by the minor cracks, which is considered acceptable and normal for the coatings as described by Vidakis et al. [42]. Moreover, the property indicates that coatings are tough and they are not damaged by deformation. On the other hand, the Cr chromized under the major critical load $L_{C3} = 15.85$ N experienced a plastic deformation followed by arc tensile cracks and beginning of a delimitation failure. Along the track, removal of material was detected (Figure 6(a)).

4. CONSLUSIONS

The results of this present study showed the effect of the addition of Magnesium as a doping element in the pack mixture of the chromized layer conducted at 1050°C. The

addition of Mg caused substantial changes in the microstructure, resulting in a crystalline structure without pores, cracks or rough particles. As a result of the EDX analysis, there is an increased rich-chromium deposition on the surface of the doped layer, which confirms that Mg enhances the diffusion of chromium (Cr) in the surface of the AISI 430. During the chromizing process, Mg reacts as a barrier to the formation of chromium oxides such as Cr₂O₃. It is replaced by a small region of magnesium oxide reacted with Cr, which is believed to be more protective than Cr₂O₃ oxide. Moreover, intermetallic phase formation, including CrC, Cr₇C₃ and Cr₂₃C₆, was less in the doped layer than in the chromized layer. Surface characteristics studies showed a desirable improvement of the Cr-Mg layer. Furthermore, Mg addition resulted in a significant improvement in surface roughness, three times lower than the chromized surface. However, this enhancement in roughness improved resistance against scratch-induced damage, as the doped layer successfully withstood a progressive load ranging from 1N to 20N. Therefore, strength adhesion was 19.21N before failure, which is classified as HF1 quality. However, failure was observed in the form of plastic deformation without fractures, due to its high elastic recovery ratio Er = 76%. In contrast, the chromized layer revealed cracks, plastic deformation, pores, and material removal. It had a strength adhesion of 15.85 N and an elastic recovery ratio of about Er = 57%. In conclusion, adding Mg to the pack mixture of the chromized coating can enhance microstructure, roughness and adhesion characteristics.

5. ACKNOWLEDGMENT

We like to express our gratitude to the Laboratory of Materials Physics and Optics (LPMO), and the Research Institute for Materials Science and Engineering, University of Mons (*Belgique*) for the scientific collaboration. This work was supported by the Corrosion, Protection and Durability of Materials Division of the Research center in Industrial Technologies *CRTI (Algeria)*.

6. REFERENCES

- Pérez, F., Hierro, M., Pedraza, F., Gomez, C. and Carpintero, M., "Aluminizing and chromizing bed treatment by cvd in a fluidized bed reactor on austenitic stainless steels", *Surface and Coatings Technology*, Vol. 120, (1999), 151-157. [https://doi.org/10.1016/S0257-8972\(99\)00355-2](https://doi.org/10.1016/S0257-8972(99)00355-2)
- Lin, N., Guo, J., Xie, F., Zou, J., Tian, W., Yao, X., Zhang, H. and Tang, B., "Comparison of surface fractal dimensions of chromizing coating and p110 steel for corrosion resistance estimation", *Applied Surface Science*, Vol. 311, (2014), 330-338. <https://doi.org/10.1016/j.apsusc.2014.05.062>
- Tsai, L.-C., Sheu, H.-H., Chen, C.-C. and Ger, M.-D., "The preparation of the chromized coatings on aisi 1045 carbon steel plate with the electroplating pretreatment of ni or ni/cr-c film", *International Journal of Electrochemical Science*, Vol. 10, No. 1, (2015), 317-331.
- Santander, J.A., Lopez, E., Tonetto, G.M. and Pedemera, M.N., "Preparation of ninbo/aisi 430 ferritic stainless steel monoliths for catalytic applications", *Industrial & Engineering Chemistry Research*, Vol. 53, No. 28, (2014), 11312-11319. <http://dx.doi.org/10.1021/ie501884g>
- Carvalho, C.E.R.d., Costa, G.M.d., Cota, A.B. and Rossi, E.H., "High temperature oxidation behavior of aisi 304 and aisi 430 stainless steels", *Materials Research*, Vol. 9, (2006), 393-397. <https://doi.org/10.1590/S1516-14392006000400009>
- Sabioni, A.C.S., Huntz, A.M., Salgado, M.F., Pardini, A., Rossi, E.H., Paniago, R.M. and Ji, V., "Atmosphere dependence of oxidation kinetics of unstabilized and nb-stabilized aisi430 ferritic stainless steels in the temperature range 850–950° c", *Materials at High Temperatures*, Vol. 27, No. 2, (2010), 89-96. <https://doi.org/10.3184/096034010X12710805379897>
- Lee, S., Cho, K., Lee, W. and Jang, H., "Improved corrosion resistance and interfacial contact resistance of 316l stainless-steel for proton exchange membrane fuel cell bipolar plates by chromizing surface treatment", *Journal of Power Sources*, Vol. 187, No. 2, (2009), 318-323. <https://doi.org/10.1016/j.jpowsour.2008.11.064>
- Popoola, A., Aigbodion, V.S., Fayomi, O. and Abdulwahab, M., "Experimental study of the effect of siliconizing parameters of thermochemical treatment of low carbon steel", *Silicon*, Vol. 8, (2016), 201-210. <https://doi.org/10.1007/s12633-015-9387-3>
- Dong, Z., Zhou, T., Liu, J., Zhang, X., Shen, B., Hu, W. and Liu, L., "Effects of pack chromizing on the microstructure and anticorrosion properties of 316l stainless steel", *Surface and Coatings Technology*, Vol. 366, (2019), 86-96. <https://doi.org/10.1016/j.surfcoat.2019.03.022>
- Ganji, O., Sajjadi, S.A., Yang, Z.G., Mirjalili, M. and Najari, M.R., "On the formation and properties of chromium carbide and vanadium carbide coatings produced on w1 tool steel through thermal reactive diffusion (trd)", *Ceramics International*, Vol. 46, No. 16, (2020), 25320-25329. <https://doi.org/10.1016/j.ceramint.2020.06.326>
- Leferink, R. and Huijbregts, W., "Chromium diffusion coatings for the protection of low-alloy steel in a sulphidizing atmosphere", *Corrosion Science*, Vol. 35, No. 5-8, (1993), 1235-1242. [https://doi.org/10.1016/0010-938X\(93\)90343-F](https://doi.org/10.1016/0010-938X(93)90343-F)
- Sen, S., "A study on kinetics of crxc-coated high-chromium steel by thermo-reactive diffusion technique", *Vacuum*, Vol. 79, No. 1-2, (2005), 63-70. <https://doi.org/10.1016/j.vacuum.2005.01.009>
- Meng, T., Guo, Q., Xi, W., Ding, W., Liu, X., Lin, N., Yu, S. and Liu, X., "Effect of surface etching on the oxidation behavior of plasma chromizing-treated aisi440b stainless steel", *Applied Surface Science*, Vol. 433, (2018), 855-861. <https://doi.org/10.1016/j.apsusc.2017.10.111>
- Bai, C.-Y., Lee, J.-L., Wen, T.-M., Hou, K.-H., Wu, M.-S. and Ger, M.-D., "The characteristics of chromized 1020 steel with electrical discharge machining and ni electroplating pretreatments", *Applied Surface Science*, Vol. 257, No. 8, (2011), 3529-3537. <https://doi.org/10.1016/j.apsusc.2010.11.070>
- Iorga, S., Ciuca, S., Leuvre, C. and Colis, S., "Influence of the thermo-chemical conditions on the carbo-chromization process of α-fe matrices obtained by powder sintering technique", *Journal of Alloys and Compounds*, Vol. 512, No. 1, (2012), 100-104. <https://doi.org/10.1016/j.jallcom.2011.09.030>
- Hu, J., Zhang, Y., Yang, X., Li, H., Xu, H., Ma, C., Dong, Q., Guo, N. and Yao, Z., "Effect of pack-chromizing temperature on microstructure and performance of aisi 5140 steel with cr-

- coatings", *Surface and Coatings Technology*, Vol. 344, (2018), 656-663. <https://doi.org/10.1016/j.surfcoat.2018.03.099>
17. Murakami, T., Hibi, Y., Mano, H., Matsuzaki, K. and Inui, H., "Friction and wear properties of the siliconized, chromized and borochromized steel substrates", in Materials Science Forum, Trans Tech Publ. Vol. 783, (2014), 1464-1469.
 18. Tarakci, M. and Guruswamy, S., "Influence of surface roughness on the coercivity and magnetic interactions in coCr_x (x= pt, pd, ta, b) thin film media", *Surface Engineering: Science and Technology II*, (2002), 283-292.
 19. Hakami, F., Pramanik, A. and Basak, A., "Duplex surface treatment of steels by nitriding and chromizing", *Australian Journal of Mechanical Engineering*, Vol. 15, No. 1, (2017), 55-72. <https://doi.org/10.1080/14484846.2015.1093256>
 20. Liu, S., Yang, J., Liang, X., Sun, Y., Zhao, X. and Cai, Z., "Investigation of the preparation, corrosion inhibition, and wear resistance of the chromized layer on the surfaces of t9 and spec steels", *Materials*, Vol. 15, No. 22, (2022), 7902. <https://doi.org/10.3390/ma15227902>
 21. Chou, C.-C., Lee, J.-W. and Chen, Y.-I., "Tribological and mechanical properties of hfcvd diamond-coated wc-co substrates with different cr interlayers", *Surface and Coatings Technology*, Vol. 203, No. 5-7, (2008), 704-708. <https://doi.org/10.1016/j.surfcoat.2008.08.055>
 22. Ghorbani, H. and Poladi, A., "Md-simulation of duty cycle and tan interlayer effects on the surface properties of ta coatings deposited by pulsed-dc plasma assisted chemical vapor deposition", *International Journal of Engineering, Transactions B: Applications*, Vol. 33, No. 5, (2020), 861-869. <https://doi.org/10.5829/ije.2020.33.05b.18>
 23. Akbarzadeh, M., Zandrahimi, M. and Moradpour, E., "A study of the tribological properties of sputter-deposited mosx/cr coatings", *International Journal of Engineering, Transactions B: Applications*, Vol. 31, No. 5, (2018), 792-798. <http://dx.doi.org/10.5829/ije.2018.31.05b.14>
 24. Ye, F., Mohammadtaheri, M., Li, Y., Shiri, S., Yang, Q. and Chen, N., "Diamond nucleation and growth on wc-co inserts with Cr₂O₃-Cr interlayer", *Surface and Coatings Technology*, Vol. 340, (2018), 190-198. <https://doi.org/10.1016/j.surfcoat.2018.02.056>
 25. Han, D., Hou, Y., Jiang, B., Geng, B., He, X., Shagdar, E., Lougou, B.G. and Shuai, Y., "Enhanced corrosion resistance of alloy in molten chloride salts by adding nanoparticles for thermal energy storage applications", *Journal of Energy Storage*, Vol. 64, (2023), 107172. <https://doi.org/10.1016/j.est.2023.107172>
 26. Chang, T.-C., Wang, J.-Y., Chia-Ming, O. and Lee, S., "Grain refining of magnesium alloy az31 by rolling", *Journal of Materials Processing Technology*, Vol. 140, No. 1-3, (2003), 588-591. [https://doi.org/10.1016/S0924-0136\(03\)00797-0](https://doi.org/10.1016/S0924-0136(03)00797-0)
 27. Wang, M., Huang, W., Shen, Z., Gao, J., Shi, Y., Lu, T. and Shi, Q., "Phase evolution and formation of λ phase in Ti₃O₅ induced by magnesium doping", *Journal of Alloys and Compounds*, Vol. 774, (2019), 1189-1194. <https://doi.org/10.1016/j.jallcom.2018.09.350>
 28. Yan, G., Yu, W. and Shengping, S., "Oxidation protection of enamel coated ni based superalloys: Microstructure and interfacial reaction", *Corrosion Science*, Vol. 173, (2020), 108760. <https://doi.org/10.1016/j.corsci.2020.108760>
 29. Fan, H.J., Gösele, U. and Zacharias, M., "Formation of nanotubes and hollow nanoparticles based on kirkendall and diffusion processes: A review", *Small*, Vol. 3, No. 10, (2007), 1660-1671. <https://doi.org/10.1002/smll.200700382>
 30. Hasibi, H., Mahmoudian, A. and Khayati, G., "Modified particle swarm optimization-artificial neural network and gene expression programming for predicting high temperature oxidation behavior of Ni-Cr-W-MO alloys", *International Journal of Engineering, Transactions B: Applications*, Vol. 33, No. 11, (2020), 2327-2338. <https://doi.org/10.5829/ije.2020.33.11b.23>
 31. Jafarnejad, E., Khanahmadzadeh, S., Ghanbary, F. and Enhessari, M., "Synthesis, characterization and optical band gap of pirochromite (MgCr₂O₄) nanoparticles by stearic acid sol-gel method", *Current Chemistry Letters*, Vol. 5, No. 4, (2016), 173-180. <http://dx.doi.org/10.5267/j.ccl.2016.7.001>
 32. Abbasi, A., Sajadi, S.M.S., Amiri, O., Hamadian, M., Moayedi, H., Salavati-Niasari, M. and Beigi, M.M., " MgCr₂O₄ and mgcr₂o₄/ag nanostructures: Facile size-controlled synthesis and their photocatalytic performance for destruction of organic contaminants", *Composites Part B: Engineering*, Vol. 175, (2019), 107077. <https://doi.org/10.1016/j.compositesb.2019.107077>
 33. Xia, F., Xu, W., Chen, L., Wu, S. and Sangid, M.D., "Generalized stacking fault energies of Cr₂₃C₆ carbide: A first-principles study", *Computational Materials Science*, Vol. 158, (2019), 20-25. doi. <https://doi.org/10.1016/j.commatsci.2018.11.006>
 34. Almubarak, A., Abuhaimed, W. and Almazrouee, A., "Corrosion behavior of the stressed sensitized austenitic stainless steels of high nitrogen content in seawater", *International Journal of Electrochemistry*, Vol. 2013, (2013). doi. <https://doi.org/10.1155/2013/970835>
 35. Wang, Z., Lu, J. and Lu, K., "Wear and corrosion properties of a low carbon steel processed by means of smat followed by lower temperature chromizing treatment", *Surface and Coatings Technology*, Vol. 201, No. 6, (2006), 2796-2801. doi. <https://doi.org/10.1016/j.surfcoat.2006.05.019>
 36. Zheng, M. and Rapp, R.A., "Simultaneous aluminizing and chromizing of steels to form (Fe, Cr) 3Al coatings", *Oxidation of Metals*, Vol. 49, No. 1-2, (1998), 19-31. doi. <https://doi.org/10.1023/A:1018870105824>
 37. Jyrkas, K., Lajunen, L., Siivari, J. and Patrikainen, T., "Diffusion nickelising and chromising of steel by chloride compounds using chemical vapour deposition in a flow reactor", *Scandinavian Journal of Metallurgy*, Vol. 19, No. 6, (1990), 288-304.
 38. NAEIMI, F. and Tahari, M., "Effect of surface morphologies on the isothermal oxidation behavior of mrcraly coatings fabricated by high-velocity oxyfuel processes", *International Journal of Engineering, Transactions C: Aspects*, Vol. 30, No. 3, (2017), 432-438.
 39. Beltrami, M., Dal Zilio, S., Kapun, G., Ciubotaru, C.D., Rigoni, F., Lazzarino, M. and Sbaizero, O., "Surface roughness control in nanolaminar coatings of chromium and tungsten nitrides", *Micro and Nano Engineering*, Vol. 14, (2022), 100107. <https://doi.org/10.1016/j.mne.2022.100107>
 40. Hou, W. and Kang, Z., "Preparation of duplex film through microarc oxidation coloring and polymer plating on mg-li alloy and its corrosion resistance", *International Journal of Electrochemical Science*, Vol. 8, No. 4, (2013), 5613-5620.
 41. Quan, C. and He, Y., "Properties of nanocrystalline cr coatings prepared by cathode plasma electrolytic deposition from trivalent chromium electrolyte", *Surface and Coatings Technology*, Vol. 269, (2015), 319-323. <https://doi.org/10.1016/j.surfcoat.2015.02.001>
 42. Vidakis, N., Antoniadis, A. and Bilalis, N., "The vdi 3198 indentation test evaluation of a reliable qualitative control for layered compounds", *Journal of Materials Processing Technology*, Vol. 143, (2003), 481-485. [https://doi.org/10.1016/S0924-0136\(03\)00300-5](https://doi.org/10.1016/S0924-0136(03)00300-5)

COPYRIGHTS

©2023 The author(s). This is an open access article distributed under the terms of the Creative Commons Attribution (CC BY 4.0), which permits unrestricted use, distribution, and reproduction in any medium, as long as the original authors and source are cited. No permission is required from the authors or the publishers.

**Persian Abstract****چکیده**

در مطالعه حاضر، اثر افزودن منیزیم (Mg) به عنوان عنصر دوپینگ بر روی مورفولوژی و ویژگی‌های سطحی لایه کرومی شده بررسی شد. برای دستیابی به این هدف، لایه‌های کرومیزه با فرآیند کرومیزاسیون در بسته‌بندی سیمانی در دمای ۱۰۵۰ درجه سانتی‌گراد پوشش داده و دوپ شدند. ضخامت لایه دوپ شده حدود ۲۶ میکرومتر بود، در حالی که کروم شده تقریباً ۲۴ میکرومتر بود. مورفولوژی سطح و ترکیب پوشش‌ها با استفاده از میکروسکوپ الکترونی روبشی (SEM) و طیف سنجی اشعه ایکس پراکنده انرژی (EDX) آنالیز شد. نتایج نشان داد که یک ساختار کریستالی را می‌توان با افزودن منیزیم به عنوان یک عنصر دوپینگ به مخلوط بسته با موفقیت رسوب کرد. بنابراین، منیزیم به عنوان یک مانع در برابر تشکیل Cr_2O_3 عمل می‌کند، که منجر به ایجاد یک منطقه کروم غنی تر و تشکیل اکسید محافظ می‌شود. علاوه بر این، کاربرد کمتری در لایه دوپ شده تشکیل می‌شود. زبری لایه با افزودن منیزیم (Mg) افزایش می‌یابد و متوسط زبری (Ra) آن ۳ برابر کمتر از کرومیزه است که به ترتیب حدود ۰.۳۱۵ میکرومتر و ۱.۰۳۹ میکرومتر است. علاوه بر این، خراش بارگذاری پیش‌رونده در N1 و N20 انجام شد. نتایج نشان داد که منیزیم در لایه کرومی شده توانایی مقاومت در برابر سطوح مختلف تنش مکانیکی را با چسبندگی استحکامی در حدود ۱۹.۲۱ نیوتن افزایش می‌دهد و می‌تواند محافظت بیشتری نسبت به کروم کروم داشته باشد.